

Distributed flexibility as a cost-effective alternative to grid reinforcement

Jordan Holweger, Christophe Ballif, Nicolas Wyrsh
Photovoltaics and thin film electronics laboratory (PV-LAB)

École Polytechnique Fédérale de Lausanne (EPFL), Institute of Electrical and Micro Engineering (IEM)
Neuchâtel, Switzerland

{jordan.holweger, christophe.ballif, nicolas.wyrsh}@epfl.ch

Abstract—The deployment of distributed photovoltaics (PV) in low-voltage networks may cause technical issues such as voltage rises, line ampacity violations, and transformer overloading for distribution system operators (DSOs). These problems may induce high grid reinforcement costs. In this work, we assume the DSO can control each prosumer’s battery and PV system. Under such assumptions, we evaluate the cost of providing flexibility and compare it with grid reinforcement costs. Our results highlight that using distributed flexibility is more profitable than reinforcing a low-voltage network until the PV generation covers 145% of the network annual energy demand.

Index Terms—PV, flexibility, grid reinforcement cost, battery, optimal power-flow

I. INTRODUCTION

The fast deployment of distributed photovoltaics (PV) causes numerous challenges to distribution system operators (DSOs). The imbalance between local generation and load can create technical problems in low-voltage grids, such as line ampacity violations, overvoltage, and transformer overloading [1]. A DSO must take countermeasures such as grid reinforcement (GR) [2], [3]. Alternatively, future distributed PV systems might provide a significant degree of flexibility to reduce the need for GR. Indeed, battery energy storage systems (BESSs) [4], inverter reactive power capability [5], [6], [7], and active power curtailment (APC) are possible solutions to increase a network’s flexibility and mitigate GR costs [8]. Recent literature demonstrated that BESSs might increase a network’s PV hosting capacity but are not competitive with GR [9], [10]. This work compares the GR cost with the cost of harvesting distributed flexibility, particularly BESS, APC, and inverter reactive power capabilities for various PV penetration levels.

II. NOTATION AND BASIC FORMULAS

This section aims to present the basic notation and symbols used in this paper. This work analyses a low-voltage grid with connected prosumers with a BESS, which are considered as static loads or generators injecting active and reactive power $P_{i,t}, Q_{i,t}$ at their grid connection points. The active power consists of the PV generation $P_{i,t}^{\text{PV}}$, the active power curtailment $P_{i,t}^{\text{cur}}$, the BESS’s exchange power $P_{i,t}^{\text{bat}}$ (positive when discharging), and the uncontrollable load $P_{i,t}^{\text{load}}$. Fig. 1 illustrates the power balance of each prosumer.

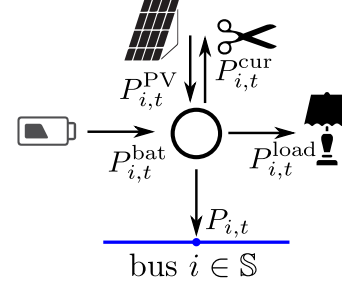


Fig. 1. System power balance.

Sets:

- $\mathbb{B}, \mathbb{L}, \mathbb{S}$ sets of buses, lines, and prosumers’ systems ($\mathbb{S} \subset \mathbb{B}$) respectively.
- \mathbb{L}^{tr} set of transformer branches (pair of bus (ik) with i the high-voltage bus).

Parameters:

- $j = \sqrt{-1}$ imaginary number.
- $P_{i,t}^{\text{load}}$ uncontrollable active power load at bus i .
- $P_{i,t}^{\text{PV}}$ PV generation at bus i .
- G_{ik}, B_{ik} conductance/susceptance on line (ik) .
- \bar{x}, \underline{x} upper and lower limit for variable x .
- x^+, x^- positive and negative part of x .
- q_r^{max} inverter reactive power capabilities ratio (MVar/MW).
- $c^{\text{imp}}, c^{\text{exp}}$ import and export tariff (consumer perspective).
- L, r component lifetime and interest rate to calculate the annualisation factor R .

Variables:

- $P_{i,t}^{\text{bat}}$, battery active power (positive when discharging).
- $P_{i,t}^{\text{cur}}$, PV active power curtailment uncontrollable active power load at bus i .
- $Q_{i,t}^{\text{PV}}$ PV inverter reactive power injection.
- S_i^{tr} transformer apparent power.
- $V_{i,t}, I_{ik,t}$ voltage magnitude at bus i and current in line (ik) and time t .
- $\theta_{ik,t}$ voltage angle difference between bus i and k at time t .

AC load flow equations:

$$P_{i,t} = \begin{cases} P_{i,t}^{\text{PV}} - P_{i,t}^{\text{cur}} + P_{i,t}^{\text{bat}} - P_{i,t}^{\text{load}} & i \in \mathbb{S} \\ 0 & i \in \mathbb{B} - \mathbb{S} \end{cases} \quad (1a)$$

$$Q_{i,t} = \begin{cases} Q_{i,t}^{\text{PV}} & i \in \mathbb{S} \\ 0 & i \in \mathbb{B} - \mathbb{S} \end{cases} \quad (1b)$$

$$P_{i,t} = V_{i,t} \sum_{k \in \mathbb{B}} V_{k,t} \left(G_{ik} \cos \hat{\theta}_{ik,t} + B_{ik} \sin \hat{\theta}_{ik,t} \right) \quad (1c)$$

$$Q_{i,t} = V_{i,t} \sum_{k \in \mathbb{B}} V_{k,t} \left(G_{ik} \sin \hat{\theta}_{ik,t} - B_{ik} \cos \hat{\theta}_{ik,t} \right) \quad (1d)$$

$$I_{ik,t} = (G_{ik} + jB_{ik}) \cdot (V_{i,t} - V_{k,t}) \quad (1e)$$

Network operation constraints:

$$\underline{V} \leq V_{i,t} \leq \bar{V} \quad \forall i \in \mathbb{B} \quad (2a)$$

$$I_{ik,t} \leq \bar{I} \quad \forall (ik) \in \mathbb{L} \quad (2b)$$

$$S_i^{\text{tr}} = |V_{i,t} \cdot I_{ik,t}| \leq \bar{S}_i^{\text{tr}} \quad \forall (ik) \in \mathbb{L}^{\text{tr}} \quad (2c)$$

III. METHODOLOGY

The methodology is based on a sequential approach. First, following the method described in [11], the BESS's capacity $E_{\text{cap}}^{\text{bat}}$ and its optimal control trajectory are optimised for each prosumer with a fixed PV penetration (fixed PV capacity for each system, $P_{\text{cap}}^{\text{PV}}$). The optimisation problem aims to minimise the total cost of ownership of each BESS-PV system (3a) composed of the sum of the annualised BESS capital cost and the system operating cost (3b), subject to the power balance (1a). The operating costs (3b) are the cost of exchanging energy with the grid under an import and export tariff (from a prosumer's perspective) c^{imp} and c^{exp} , respectively. As the PV capacity is fixed, it does not appear in the objective function. The term σ (3c) is a regularisation cost whose aim is to minimise battery usage. The annualisation factor R depends on the considered lifetime L and interest rate r . More details about the PV and BESS model can be found in [11].

Second, the load flow problem (1a)-(1e) is solved at each point in time to calculate the network variable states, $V_{i,t}$, $I_{ik,t}$, and S_i^{tr} . Then, the annualised cost of GR (4a) is calculated as the sum of the cost of replacing lines (4b) because of line ampacity violation (4d), and the cost of replacing transformers due to an apparent power limit violation (4e). The annualisation factor R^{grid} is calculated as in (3d). The cost of replacing a line is proportional to the line length d_l and its specific cost per unit of length c^{line} . The cost of replacing a transformer is simply the product of the transformer cost per unit of capacity c^{trafo} and the new maximum apparent power $\max_t S_t^{\text{tr}}$.

Third, distinct time domains $t \in \Pi_m$, $m = 1 \dots M$ are constructed in which network constraints (2a)-(2c) are not satisfied. These contiguous time steps represent intervention periods in which the DSO must undertake actions to prevent violations of network constraints. To model these actions, we solve an optimal power-flow problem for each period Π_m with the goal of minimizing the PV curtailed energy (5a), which determines where and when to charge or discharge the

batteries, inject or absorb reactive power (within the inverter capability, q_r^{max} constraints (5c)), and perform APC. Due to the multi-period nature of this problem, any action altering the battery state of the charge profile may have consequences in the future. To prevent such distortion, the BESS's energy content at the beginning and end of the intervention period should match the original energy content from the optimal control trajectory (5b). We implemented this constraint in the POWERMODELS [12] library that we used to solve the optimal power-flow problem. Note that the BESS model is slightly different in POWERMODELS than in [11]. Typically in the former implementation, we neglected the active power losses, did not consider injection impedance, and assumed that the battery cannot provide reactive power.

Finally, the cost of providing flexibility is defined as the difference between the operating costs evaluated after solving (5a) $OPEX'_i$ and the original operating cost $OPEX_i$ from optimal control trajectory (3a). The methodology is graphically summarised in Fig. 2. We further distinguish the case where storage is available and can be controlled by the DSO from the case where no storage is available. In the latter case P^{bat} is removed from the power balance, and PV curtailment and reactive power injection are the only options available to the DSO.

$$\min_{E_{\text{cap}}^{\text{bat}}, P^{\text{bat}}} OPEX + \sigma + R \cdot (c_F^{\text{bat}} + c^{\text{bat}} \cdot E_{\text{cap}}^{\text{bat}}) \quad (3a)$$

$$OPEX = \sum_{t=1}^T \left(P_t^- \cdot c_t^{\text{imp}} - P_t^+ \cdot c_t^{\text{exp}} \right) \quad (3b)$$

$$\sigma = \sum_{t=1}^T P^{\text{+bat}} \cdot 10^{-6} \quad (3c)$$

$$R = \frac{r \cdot (1+r)^L}{(1+r)^L - 1} \quad (3d)$$

$$C_{\text{reinf}} = R^{\text{grid}} \cdot (C_{\text{reinf, line}} + C_{\text{reinf, trafo}}) \quad (4a)$$

$$C_{\text{reinf, line}} = \sum_{(l) \in \mathbb{L}} \delta_l \cdot c^{\text{line}} \cdot d_l \quad (4b)$$

$$C_{\text{reinf, trafo}} = \delta_{tr} \cdot c^{\text{trafo}} \cdot \left(\max_t S_t^{\text{tr}} \right) \quad (4c)$$

$$\delta_l = \begin{cases} 1 & \text{if } \max_t I_{l,t} > I^{\text{max}} \\ 0 & \text{otherwise} \end{cases} \quad (4d)$$

$$\delta_{tr} = \begin{cases} 1 & \text{if } \max_t S_t^{\text{tr}} > S^{\text{tr, max}} \\ 0 & \text{otherwise} \end{cases} \quad (4e)$$

$$\min_{P_{i,t}^{\text{cur}}, P^{\text{bat}}, Q_{i,t}^{\text{PV}}} \sum_{i \in \mathbb{S}, t \in \Pi_m} P_{i,t}^{\text{cur}} \quad (5a)$$

$$E_{i,t}^{\text{', bat}} = E_{i,t}^{\text{bat}} \quad \text{for } t = \{\underline{\Pi}_m, \bar{\Pi}_m\} \quad i \in \mathbb{S} \quad (5b)$$

$$-q_r^{\text{max}} \cdot P_{\text{cap}, i}^{\text{PV}} \leq Q_{i,t}^{\text{PV}} \leq q_r^{\text{max}} \cdot P_{\text{cap}, i}^{\text{PV}} \quad (5c)$$

$$\Delta OPEX = \sum_i OPEX'_i - OPEX_i \quad (6)$$

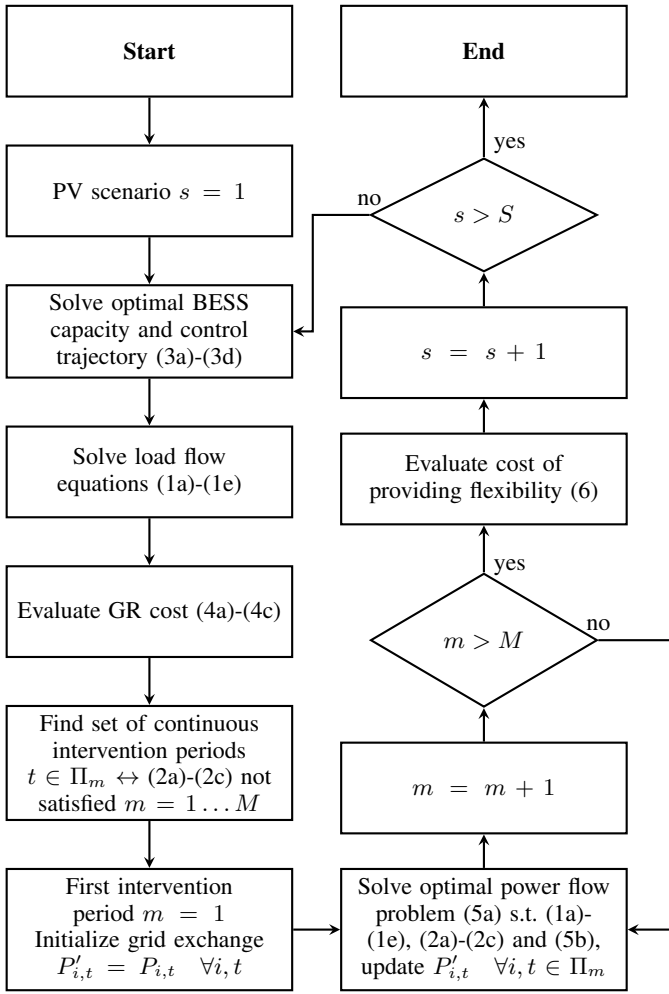


Fig. 2. Workflow of the methodology.

IV. CASE STUDY

The *CIGRE* low-voltage network [13], depicted in Fig. 4, serves as our test case. Loads and PV generation profiles cover one year at 15-min resolution. The load profiles come from an internal load database acquired over several projects [14], [15]. They have been allocated to each network bus, minimising the sum of the differences between the *CIGRE* loads' apparent power and the 99th quantile of the internal load profiles. Similarly, the roofs' characteristics that give the PV potential capacity are drawn from a building database from the Swiss building registry¹, minimising the sum of the differences between the annual allocated electricity demand and the building estimated electricity demand. The annual energy demand and maximum PV potential capacity for each prosumer are listed in Table I. The total annual energy demand and PV capacities are 1050 MWh and 1500 kW, respectively.

Each prosumer's BESS capacity and control trajectory is optimised using a time-of-use tariff reported in Table II. The import rate is $23.92 \frac{\text{cts}}{\text{kWh}}$ during peak hours and $15.16 \frac{\text{cts}}{\text{kWh}}$

during off-peak hours. The export rate is $8.16 \frac{\text{cts}}{\text{kWh}}$ all the time. The cost of a BESS c^{bat} is assumed to be $182 \frac{\text{CHF}}{\text{kWh}}$, with a fixed component $c_F^{\text{bat}} = 0$, as reported in Table III. The BESS capacities reported in Table I correspond to the optimised capacities at the maximum PV capacity.

The number of modules giving the maximum potential PV capacity for each system is scaled by an arbitrary number (reported in red in Fig. 5) to construct various PV penetration scenarios. The number of modules is then rounded to the nearest integer. To prevent an unrealistically small installation, we assume that if the resulting PV levelised cost of electricity is greater than a threshold of $23.92 \frac{\text{cts}}{\text{kWh}}$ (corresponding to the high import rate), the resulting PV capacity is set to zero for this scenario. The PV levelised cost of electricity is calculated assuming a PV lifetime of 25 years, a discount rate of 3%, a PV cost of $83 \frac{\text{cts}}{\text{W}}$, and a fixed cost of 10'050 CHF. This process is graphically summarised in Fig. 3. The PV and battery capacity indicated in Fig. 4 and Table I corresponds to the maximum PV penetration scenario (scale = 100%). The global horizontal and diffuse irradiance data are extracted from a weather station in Pully².

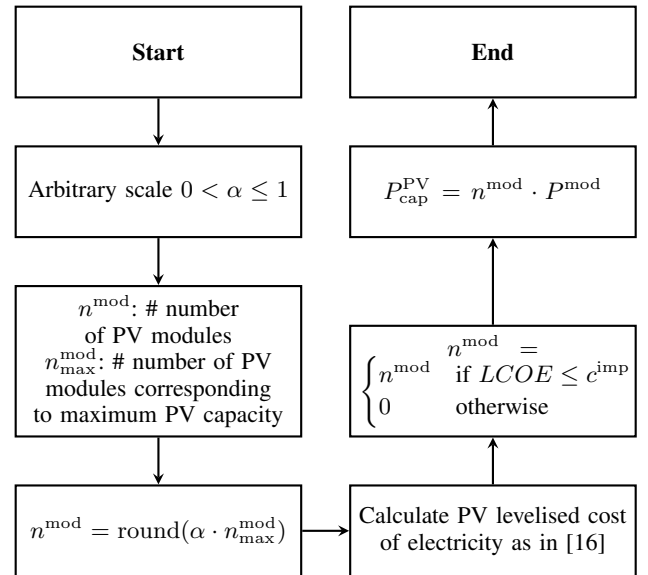


Fig. 3. Determination of the installed PV capacity for a particular system.

We assumed the costs for GR of the transformer and lines are $60 \frac{\text{kCHF}}{\text{MVA}}$ and $70 \frac{\text{kCHF}}{\text{km}}$. The transformer's and lines' lifetime is assumed to be 30 years, as reported in Table III.

V. RESULTS

Fig. 6 illustrates a typical operating day of the maximum PV penetration scenario. As the total PV generation increases, the C0-C1 transformer's apparent power exceeds the rated capacity (transformer loading above 100% in Fig. 6a). Similarly, the voltage level exceeds 1.05 pu in bus C13. This is caused by an excess of PV energy, as illustrated in Fig. 6b for the system

¹<https://www.housing-stat.ch/fr/accueil.html>

²Data available at <https://gate.meteoswiss.ch/idaweb>

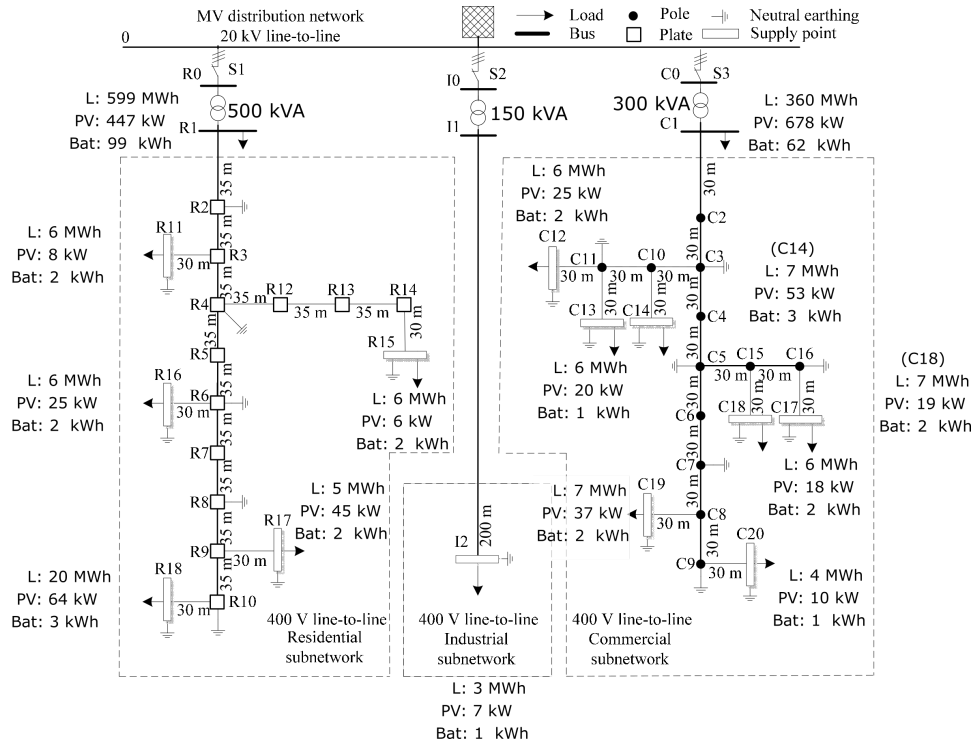


Fig. 4. Illustration of the CIGRE low-voltage network adapted from [13].

TABLE I
SYSTEMS DATA

	Annual demand (MWh)	PV max capacity (kW)	Battery capacity (kWh)
R1	598.97	447.09	141.13
R11	6.09	8.19	2.89
R15	6.13	6.30	2.18
R16	5.58	24.89	2.48
R17	5.29	44.74	2.30
R18	19.82	64.27	4.71
I2	2.88	6.93	1.21
C1	360.34	678.35	87.96
C12	5.89	19.53	1.39
C13	11.73	40.64	4.83
C14	7.02	53.25	3.69
C17	5.84	17.64	2.37
C18	6.56	18.90	3.10
C19	7.34	36.86	2.65
C20	3.59	10.08	1.09
Total	1053.08	1477.69	263.97

TABLE II
TARIFF

	Hours	Tariff (cts/kWh)
c_{imp}^i	Mon-Fri 06h-22h	23.92
	Mon-Fri 22h-06h	15.16
	Sat-Sun all-day	15.16
c_{exp}		8.16

located in bus C1. To resolve such problems, a significant fraction of the PV energy needs to be curtailed, and the battery

TABLE III
SYSTEM, NETWORK, AND BATTERY PARAMETERS

Param.	Unit	Value
T	-	35040
T^S	s	900
L	years	9
r	-	0.03
V, \bar{V}	pu	0.95-1.05
\bar{I}	kA	1
\bar{S}^{trafo}	kVA	see Fig. 4
c_{trafo}^{trafo}	kCHF/MVA	60
c_{line}^{line}	kCHF/km	70
r_{grid}	-	0.03
L_{grid}	years	30
c_{bat}^{bat}	CHF/kWh	182
c_F^{bat}	CHF	0
q_r^{max}	MVAr/MW	0.4

power profile is modified compared to its original trajectory (see Fig. 6c for the same system). The corresponding battery state of charge trajectory is kept untouched except during the intervention period, as depicted in Fig. 6d.

In the previous example, the intervention period is about 10 hours long. Fig. 7 shows the distribution of the duration of the intervention periods as well as the total duration of the interventions. As PV penetration increases, the intervention duration tends to increase. The total duration of the interventions increases to about 1300 hours (4 hours per day on average). No significant difference is observed between the case with storage and the case without storage. Table IV

reports the number of hours when the transformer experiences overloading and buses experience overvoltage. No line overloading is observed. Transformer overloading is observed starting at a PV penetration of 70%. It occurs for 5 hours only. Bus overvoltage occurs starting at a PV penetration of 119% and the cumulative time is about 30 hours. The differences between the case with storage and the case without storage are insignificant. These results highlight that, for this network, the limiting component is the transformer loading. This can be easily solved by curtailing PV energy.

As reported in Table V, an insignificant fraction of the total PV energy needs to be curtailed at a PV penetration of 70%. At the maximum PV penetration and considering no storage, 8.4% of the 1660 MWh needs to be curtailed. Using storage reduces this quantity to 2.9%. The amount of curtailed PV energy impacts the financial performance of the systems.

The cost of providing flexibility is reported in Fig. 8. As it reduces the amount of curtailed PV energy, storage significantly reduces the cost of flexibility. This cost has to be compared with the GR cost. As no line-overloading is observed, we perform a sensitivity analysis on the transformer specific cost around its nominal value ($60 \frac{\text{kCHF}}{\text{MVA}}$). For an optimistic case where the transformers cost $12 \frac{\text{kCHF}}{\text{MVA}}$, using distributed flexibility is profitable up to a PV penetration of 110%. This break-even point moves to 145% for a $60 \frac{\text{kCHF}}{\text{MVA}}$ transformer. Above such a price, it is always profitable to utilise distributed flexibility for all PV penetrations.

VI. DISCUSSION

The results highlight that distributed flexibility is profitable over GR for a significant range of PV penetrations. Several underlying assumptions need to be discussed. First, both PV and storage investment costs are assumed to be undertaken by the prosumers. We do not tackle the question of the optimal sizing of BESS and PV systems as in [17] but fix the PV capacity to generate a realistic PV penetration scenario and only solve the optimal BESS capacity problem instead. At this stage, grid support activities like PV curtailment and deviation of the BESS's optimal control trajectory are not considered as future revenue. Thus, we assume that the DSO itself does

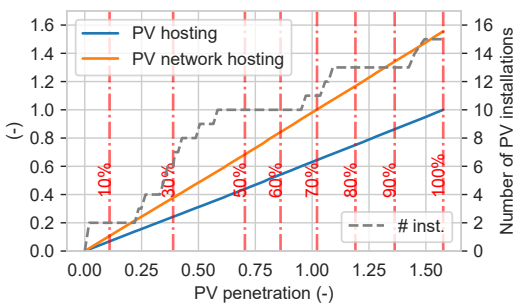
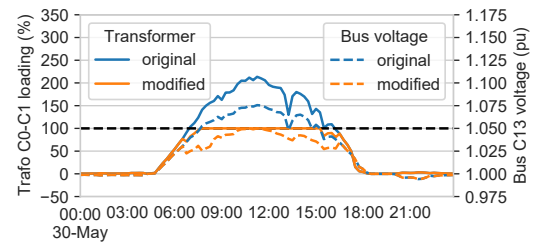
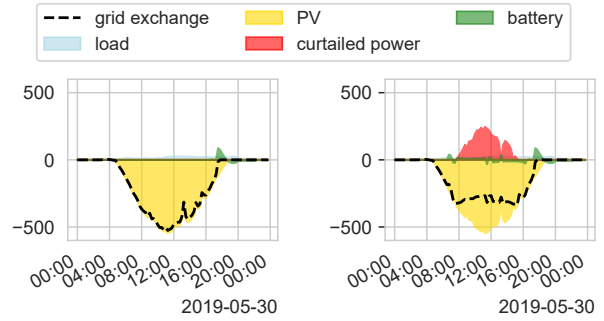


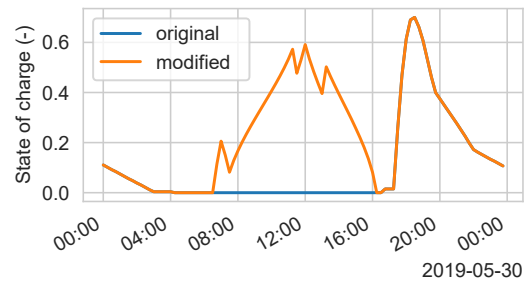
Fig. 5. PV hosting and PV network hosting ratio (left axis) and the number of installed systems (right axis, maximum is 15 systems). The red dashed lines are the selected PV penetration scenarios. The numbers indicated in red are the scale used to vary the PV capacity.



(a) Transformer loading level and bus voltage.



(b) Original system operation. (c) Modified system operation.



(d) State of charge evolution during a day.

Fig. 6. Illustration of the network and one system active power for one day, for the 100% PV capacity scenario.

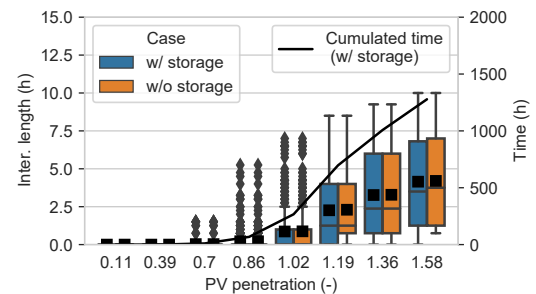


Fig. 7. Duration distribution (left axis). Averages are indicated with a square and outliers with a diamond. The total intervention time is on the right axis.

not undertake the risk of investing in distributed storage. This discards the question of the profitability of BESSs for such a grid support application as addressed by [9], [10].

A second strong assumption is buried in the BESS's optimal control trajectory. Such optimisation problems assume a perfect forecast of the uncontrollable load and PV generation.

TABLE IV
SUMMARY OF THE NETWORK VIOLATIONS FOR THE CASE WITH STORAGE.
ANY DIFFERENCES BETWEEN THE CASE WITHOUT AND WITH STORAGE
ARE INDICATED BETWEEN BRACKETS.

	Transformer overloading		Bus overvoltage	
	time (h)	max (%)	time (h)	max (pu)
PV penetration	11%	-	-	-
	39%	-	-	-
	70%	5	110	-
	86%	44	134	-
	102%	173(+2)	158	-
	119%	523(+7)	186	29(+1)
	136%	799(+5)	215	439(+3)
	158%	1044(+16)	246	846(+6)

TABLE V
ENERGY CURTAILED AND PV PRODUCTION

	Energy curtailed (%)		Generation (MWh)
	w/ storage	w/o storage	
PV penetration	11%	0.0	115
	39%	0.0	409
	70%	0.0	742
	86%	0.0	907
	102%	0.0	1076
	119%	0.3	1253
	136%	0.9	1435
	158%	2.9	1660

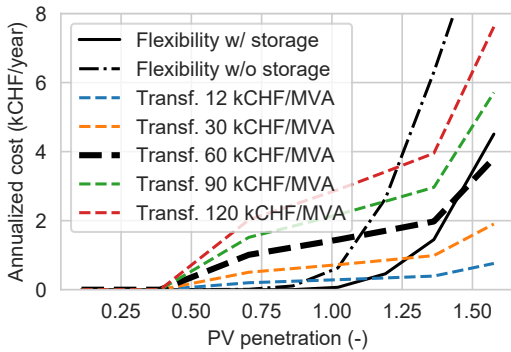


Fig. 8. Annual cost of providing flexibility versus grid reinforcement.

Similarly, the optimal power-flow problem also relies on a similar assumption. To turn such a concept into practice, there is a need for dedicated control algorithms that take load and generation uncertainties into account and that minimise future impacts on individual system operation.

Third, the costs of providing flexibility and GR are compared by annualising the operating and investment costs. This implies that the system would operate identically for the following 30 years without considering the future evolution of the technology cost and PV deployment. Our approach must be seen as an evaluation tool to estimate where GR should be undertaken, typically in networks with a high PV penetration potential. Future work may repeat such a study for a wider range of networks with different topologies and load characteristics and extract insights to better understand the profitability of distributed flexibility.

Finally, we neglected the additional cost of remote control of the prosumers. Those costs can be covered by the savings the DSO makes from using distributed flexibility instead of GR. From another perspective, those savings could be redistributed to the prosumers as a reward for contributing to the network flexibility. As a potential approach, one could define the flexibility capacity P_{cap}^{flex} as the sum of the PV and BESS's power capacity (curtailment and charging can be seen as virtual loads). The difference between the GR and the cost of flexibility in Fig. 8 corresponds to the DSO's savings, which could be redistributed to prosumers according to their flexibility capacity. The value of the flexibility capacity could be defined as:

$$C^{flex,value} = \frac{C_{reinf} - \Delta OPEX}{R_{grid}} \cdot \frac{1}{\sum_i P_{cap}^{flex}} \quad (7)$$

This quantity can be seen as a one-time subsidy to the prosumer's system. The value of the flexibility capacity is reported in Fig. 9. The flexibility capacity value decreases more significantly without storage. For a typical reinforcement cost of $60 \frac{kCHF}{MVA}$, such value lies in 20-30 CHF/kW, which corresponds to about 5-10% of the 420 CHF/kW Swiss PV one-time subsidy³.

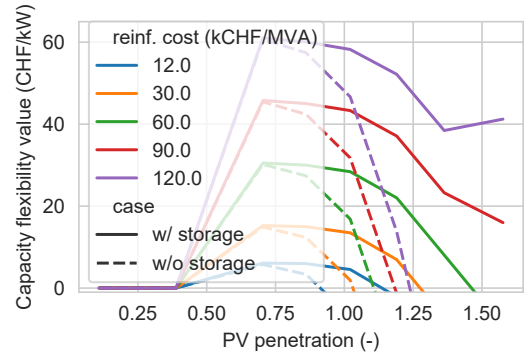


Fig. 9. Flexibility capacity value.

VII. CONCLUSION

This work aims to complement the recent literature on how to price and reward flexibility. We presented an approach to assess the cost of distributed flexibility and grid reinforcement in a low-voltage network for several PV penetration levels. Our approach starts with optimising the BESS's capacity and optimal control trajectory for each prosumer located in the network. The PV capacity is fixed to control the PV penetration at the network scale but could be included in the optimisation problem. The second step is to solve the load flow equations to evaluate potential violations of network constraints (bus overvoltage, line ampacity violation, and transformer overloading). At this stage, we evaluate the cost of grid reinforcement. Then for each continuous period

³Appendix 2.1, ch2.3 of OEnER https://www.fedlex.admin.ch/eli/cc/2017/766/fr#lv1_d1384e202/lv1_d1384e203/lv1_2

when violations of constraints were observed, we solved an optimisation problem aiming to minimise the amount of curtailed PV energy. This mimics an action undertaken by the DSO to keep the network safe. As this action is a deviation of the prosumers' optimal control trajectory, the associated cost overrun is paid to the prosumers. These cost overruns are considered to be the cost of providing flexibility. We compared the cost of grid reinforcement and providing flexibility. Distributed flexibility is more profitable than grid reinforcement when the need for grid reinforcement arises. We showed that a BESS significantly lowers the cost of providing flexibility compared to considering only PV curtailment. The BESS's profitability is ensured by the definition of the objective function of the first-stage optimisation, which minimises the prosumer's energy bill. Such a scheme transfers the risk of investing in a BESS from the DSO to the prosumers, assuming a sufficient incentive, e.g. an electricity tariff, exists to encourage the latter to invest in such technology. Future work may consider more-advanced electricity tariffs and evaluate how a DSO could select the most appropriate tariff to encourage investment in flexibility capacity and to lower the distributed flexibility cost. We also discussed a fair approach to reward flexibility as a one-time contribution to the prosumer's system. Finally, we showed that distributed flexibility is more profitable than grid reinforcement for PV penetration up to 110-145%.

Future work should focus on control algorithms taking into account load and PV generation uncertainties. Possible deployment schemes for a practical application should also be investigated.

REFERENCES

- [1] R. Viral and D. K. Khatod, "Optimal planning of distributed generation systems in distribution system: A review," *Renewable and Sustainable Energy Reviews*, vol. 16, pp. 5146–5165, 2012. [Online]. Available: https://ac.els-cdn.com/S1364032112003498/1-s2.0-S1364032112003498-main.pdf?{}_tid=1a77bac0-150b-433b-b132-14e5445f007f&acdnat=15245658111_0d26ba10fe49eb9777e61ed733dae58b
- [2] A. Scheidler, L. Thurner, and M. Braun, "Heuristic optimisation for automated distribution system planning in network integration studies," *IET Renewable Power Generation*, vol. 12, no. 5, pp. 530–538, mar 2018.
- [3] T. Vu, "A stochastic methodology to determine reinforcement cost of power distribution grid for integrating increasing share of renewable energies and electric vehicles," *International Conference on the European Energy Market, EEM*, vol. 2018-June, 2018.
- [4] N. Hashemipour, T. Niknam, J. Aghaei, H. Farahmand, M. Korpas, M. Shafie-Khah, G. J. Osorio, and J. P. S. Catalao, "A linear multi-objective operation model for smart distribution systems coordinating tap-changers, photovoltaics and battery energy storage," in *2018 Power Systems Computation Conference (PSCC)*. IEEE, jun 2018.
- [5] F. Olivier, P. Aristidou, D. Ernst, and T. Van Cutsem, "Active Management of Low-Voltage Networks for Mitigating Overvoltages Due to Photovoltaic Units," *IEEE Transactions on Smart Grid*, vol. 7, no. 2, pp. 926–936, 2016.
- [6] F. Olivier, "Solutions for integrating photovoltaic panels into low-voltage distribution networks," Ph.D. dissertation, Liège Université, 2018.
- [7] G. Prionistis, T. Souxes, and C. Vournas, "Voltage stability support offered by active distribution networks," *Electric Power Systems Research*, vol. 190, 2021.
- [8] K. Spiliotis, A. I. R. Gutierrez, and R. Belmans, "Demand flexibility versus physical network expansions in distribution grids," *Applied Energy*, vol. 182, pp. 613–624, nov 2016.
- [9] R. Gupta, F. Sossan, and M. Paolone, "Countrywide PV hosting capacity and energy storage requirements for distribution networks: The case of switzerland," *Applied Energy*, vol. 281, p. 116010, jan 2021.
- [10] R. Gupta, A. Pena-Bello, K. N. Streicher, C. Roduner, Y. Farhat, D. Thöni, M. K. Patel, and D. Parra, "Spatial analysis of distribution grid capacity and costs to enable massive deployment of PV, electric mobility and electric heating," *Applied Energy*, vol. 287, p. 116504, apr 2021.
- [11] L. Bloch, J. Holweger, C. Ballif, and N. Wyrsh, "Impact of advanced electricity tariff structures on the optimal design, operation and profitability of a grid-connected PV system with energy storage," *Energy Informatics*, vol. 2, no. 1, p. 16, 2019.
- [12] C. Coffrin, R. Bent, K. Sundar, Y. Ng, and M. Lubin, "Powermodels.jl: An open-source framework for exploring power flow formulations," in *2018 Power Systems Computation Conference (PSCC)*, June 2018, pp. 1–8.
- [13] K. Strunz, C. Abbey, C. Andrieu, R. C. Campbell, and R. Fletcher, "Benchmark Systems for Network Integration of Renewable and Distributed Energy Resources," CIGRE, Tech. Rep. July, 2009.
- [14] L. Perret, J. Fahrni, N. Wyrsh, Y. Riesen, S. Puddu, S. Weber, and D. Pfacheco Barzallo, "FLEXI Determining the flexibilization potential of the electricity demand," Federal office for energy, Tech. Rep., 2015.
- [15] L. Perret, Y. Chevillat, N. Wyrsh, L. Bloch, J. Holweger, S. Weber, and M. Péclat, "Flexi 2 Déterminer le potentiel de flexibilisation de la demande d'électricité des ménages," Federal office for energy, Tech. Rep., 2019.
- [16] C. S. Lai and M. D. McCulloch, "Levelized cost of electricity for solar photovoltaic and electrical energy storage," *Applied Energy*, vol. 190, pp. 191–203, mar 2017.
- [17] J. Holweger, L. Bloch, C. Ballif, and N. Wyrsh, "Mitigating the impact of distributed PV in a low-voltage grid using electricity tariffs," *Electric Power Systems Research*, vol. 189, p. 106763, 2020. [Online]. Available: <https://www.sciencedirect.com/science/article/pii/S0378779620305666>